GJPB

Research Article

Comparison of in-silico and in-vitro studies of benzimidazole-oxothiazolidine derivatives as m. Tubcerculosis transcriptor inhibitors

Sonal Dubey¹*, Sakshi Bhardwaj², Prabitha Prabhakaran³, Subhankar Parboth Mandal³, Ekta Singh⁴

¹College of Pharmaceutical Sciences, Dayanand Sagar University, Kumaraswamy Layout, Bengaluru, India.

²Krupanidhi College of Pharmacy, Carmelaram, Bengaluru, India.

³JSS College of Pharmacy, SS Nagar Bannimantap, Mysuru, India.

⁴Acharya & BM Reddy College of Pharmacy, Soldevanahalli, Bengaluru, India.

*Correspondence: drsonaldubey@gmail.com

Abstract

Novel *N*-(4-alkyl-4-oxo-1,3-thiazolidin-3-yl)-2-(5-nitro-1*H*-benzimidazole-1-yl)acetamide derivatives were evaluated as *M. tuberculosis* transcription inhibitors using protein 3Q3S, by performing molecular docking and molecular dynamics studies. Twelve promising candidates exhibiting good binding interactions in the form of hydrogen bonds, pi-cation interactions, pi-pi stacking and low binding energies (-7.576 kcal/mol to -5.038 kcal/mol) were selected for wet lab synthesis. Their *in-vitro* anti-tubercular activity tests using Microplate Alamar Blue Assay were compared with *in-silico* studies. Compounds **4a, 4b, and 4g** have exhibited good activity with MIC values of 1.6 μg/ml, while the other compounds exhibited activity at MIC values of 3.125-6.25 μg/ml. The results show that the presence of an additional H-bonding group at the ortho position in the substituted aryl group attached to the thiazolidine ring is leading to an increase in the activity owing to an increase in the binding interaction of the molecule to the substrate.

Introduction

Mycobacterium tuberculosis is responsible for one of the oldest documented infectious diseases-tuberculosis (TB). TB is still a major disease in developing tropical nations. Off late, there has been a resurgence of TB cases attributed to Multiple Drug- Resistant Tuberculosis (MDR-TB) and HIV infection leading to inefficient management [1]. As per WHO 2020 reports, almost 1.5 million individuals died worldwide because of TB, the second leading cause of infectious deaths after covid-19. The resistance that develops in TB can be due to rifampicin-resistant TB (RR-TB) and MDR-TB. In the world, 2/3 of the total TB cases come from 8 countries, with India having the highest count, followed by China, Indonesia, Philippines, Pakistan, Nigeria, Bangladesh and South Africa [2].

The most popular regimen for treating tuberculosis consists of four first-line drugs for at least six months: isoniazid, rifampicin, ethambutol, and pyrazinamide. The USFDA has approved bedaquiline, an ATP-synthase inhibitor, as the first medication for MDR-TB. This approval is thought to mark the beginning of a new era in TB therapy [3]. After that, several other candidates, such as Pretomanid, Delamanid, Moxifloxacin, and Linezolid, have been recently approved by FDA, and their combination therapy is under review by WHO [4]. The demand for new scaffolds that work against sensitive and resistant MTB still persists [5]. Therefore, a current focus of study, especially for the affected countries, is identifying and developing novel anti-tubercular medicines with low toxicity profiles and having potency against both drug-susceptible and drug-resistant MTB.

Benzimidazole/benzoglyoxaline scaffolds are one of the versatile structures in medicinal chemistry, encompassing extensive biological activities such as antihistaminic [6], antiulcer [7], anti-tubercular [8], antioxidant [9], antiparasitic [10], anti-inflammatory [11], analgesic [12], antimicrobial [13], antiprotozoal [14] antihypertensive [15] and anticancer activities [16]. The imidazole group (biologically active pharmacophore of the heterocyclic compound), which inhibits lipid biosynthesis, has a favorable pharmacokinetic profile and partition coefficient that affect the drug's ability to reach the target and exert efficacy against resistant TB [17]. Recent studies using benzimidazole derivatives to treat TB have come up with positive outcomes, supporting the idea that benzimidazole could potentially be a lead compound in discovering new anti-TB agents.

On the other hand, oxo-thiazolidine derivatives are also an important class of heterocyclic compounds used in novel drug design as they have proved their usefulness in various kinds of disease such as antimicrobial [18], anti-tubercular [19], antifungal, antioxidant activities and anti-HIV activities [20]. After an in-depth literature search, it was observed that more efforts have yet to be made to combine these moieties in a single molecular scaffold and design new candidates with potency and selectivity towards *M. tuberculosis*. Based on the aforementioned findings, we herein report the *in-silico* studies, the *in-vitro* activity and the comparison of results of *in-silico* and *in-vitro* study of a novel series of *N*-[(4-oxo-2-substituted aryl-1,3-thiazolidine)-acetamidyl]-5-nitro benzimidazoles derivatives as *M. tuberculosis* transcriptor inhibitors.

Materials and Methods

Molecular docking studies were performed by using Schrodinger's Maestro program 10.5. The crystal structure of the transcription protein in *Mycobacterium tuberculosis* (PDB ID: 3Q3S), having a resolution 2A0, was taken for the *in-silico* studies. Docking studies of the prepared ligands were done of the optimized protein grid using the extra precession (XP) module of Schrodinger's Maestro program.

Molecular Dynamics (MD) simulations were performed on the protein (3Q3S) and docked complexes of 3Q3S-ligand (Compound **4a** and Compound **4b**) using GROMACS version 4.5.5.

In-Silico studies

Molecular docking studies

Molecular docking studies were done by using Schrodinger's Maestro program 10.5. The crystal structure of *Mycobacterium tuberculosis* transcription inhibitor (PDB ID: 3Q3S) with a 2.0 Å resolution was used in the study. Protein structure 3Q3S was refined using the Protein preparation module. The ligand structures were drawn using an inbuilt 2D sketcher of Maestro. The ligands were optimized for docking using the LigPrep module, where the structures were converted into 3D, and then the energy minimization & optimization was done using the OPLS3 force field. The pH of the simulated environment was maintained between 7±2. The docking grid was generated using Glide Grid Module. Molecular docking studies were conducted to find the interactions between protein and predicted molecules. The prepared ligands were docked into the optimized protein grid using the extra precession (XP) module of Schrodinger's Maestro program.

Molecular Dynamics Simulation Studies

Molecular dynamics (MD) simulation studies were performed for the *M. tuberculosis* transcription inhibitor protein with PDB ID: 3Q3S and docked complexes of 3Q3S-ligand (Cpd 4a and INH). CHARMM 27 was assigned the force field, and dynamics calculations were done with GROMACS version 4.5.5. Swiss Param was used to generating CHARMM parameters for all the ligands and the various topology descriptors [21]. A cut-off distance of 1.0 nm was fixed for calculating van der Waal interactions. Partial Mesh Ewald (PME) summation with a cut-off of 1 nm was applied for long-range electrostatics columbic interaction calculations. The inclusion of counter ions was made to maintain the electro-neutrality of the system. TIP3P water model was used to solvation the system, and simulations were performed by keeping the protein atoms 1.5 nm apart from triclinic box walls [22]. The system's energy was minimized using the steepest descent algorithm with a 1000 KJ/mol/nm tolerance. Canonical

NVT ensembles followed by NPT were used to simulate system equilibrium by applying position restraints on the complex. The equilibration simulations were run at 200 ps each at a temperature of 300 K and pressure of 1 bar. Initial velocities generation was done per Maxwell distribution, and velocity rescaling was done to perform temperature coupling with a coupling constant of 0.1 ps. Temperature-pressure coupling was carried out using the extended ensemble Parrinello-Rahman method and a coupling constant of 2 ps [23]. The production runs for 10 ns were then applied to the equilibrated system. It was integrated across a time step of two fs. The trajectories were stored every 500 steps, and the XMGRACE-5.1.22 program and GROMACS analysis tools were used to examine them [24]. Anti-TB activity of the 12 selected compounds was taken from the literature, a previous work carried out by our lab [25].
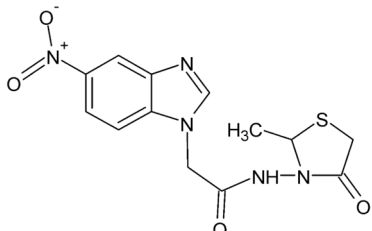
Anti-tubercular activity

The antimycobacterial activity of synthesized compounds against *M. tuberculosis* was assessed using the Alamar Blue Assay (MABA) microplate. Vaccine strain, H37 RV strain) ATCC No- 27294 of *Mycobacteria tuberculosis* was used for this study. Standards values of Pyrazinamide- 3.125 µg/ml, Ciprofloxacin-3.125 µg/ml and Streptomycin- 6.25 µg/ml were considered for anti-TB activity.
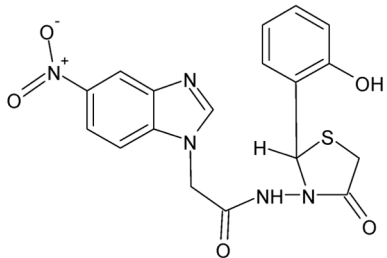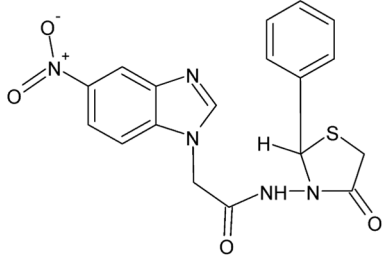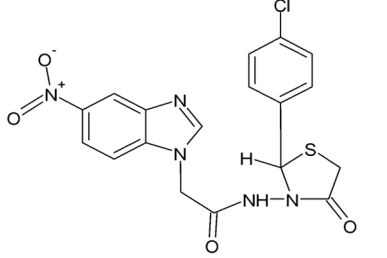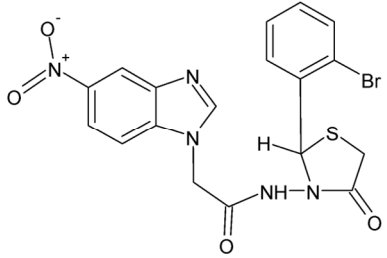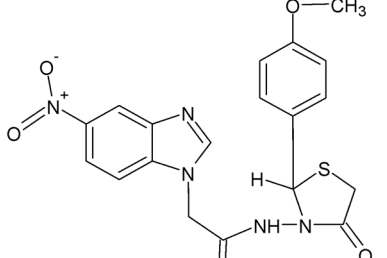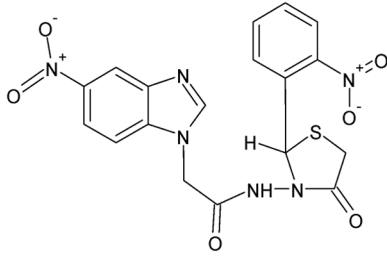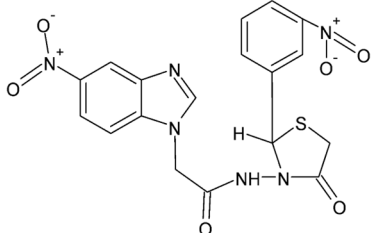
Results and Discussion
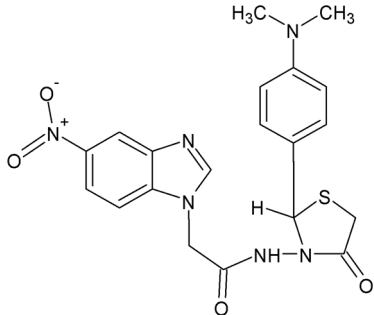
Molecular docking

Around 105 compounds were designed as *N*-[(4-oxo-2-substituted aryl-1,3-thiazolidine)-acetamidyl]-5-nitro benzimidazoles derivatives. These structures were subjected to *in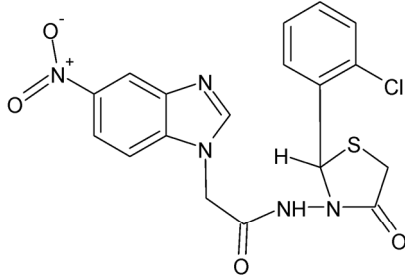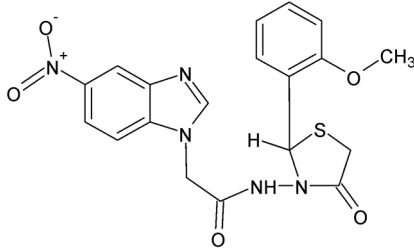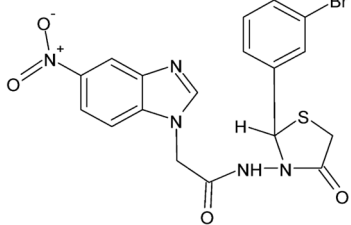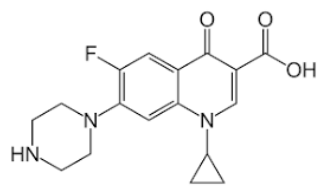-silico* studies using Schrodinger's Maestro program 10.5. Docking studies were performed using M. tuberculosis transcription inhibitor protein PDB ID 3Q3S. The protein has a XRD resolution of $2A^0$ and contained co-crystallized ligand (2-(2-methylphenoxy)-*N*-[2-(4-methylphenyl)-2*H*-benzotriazol-5-yl] acetamide), in the active site. The ligand was first removed from the active site, and protein was prepared for docking studies. Docking studies compressed our search to 12 compounds from the pool, which exhibited good binding interactions and energies. These compounds exhibited scores ranging from -7.576 kcal/mol to – 5.038 kcal/mol by forming hydrogen bonds, pi-cation interactions and pi-pi stacking. Ciprofloxacin, the reference compound, showed -6.714 kcal/mol binding energy with the same protein. Figure **1a, 1b; 2a, 2b; and 3a, 3b** show the docked pose and ligand interaction diagrams for molecules **4a, 4b, and 4g,** respectively**.** The amino acids ASN179, ASN176, PHE110, LEU90, TYR148, and TRP145 interact with ligands in the binding cavity. The docking results regarding binding energy, hydrogen bonding and binding interactions were interpreted. The compound **4a**, which showed the best binding energy (-7.576 kcal/mol), has an electron-donating group attached to methyl-oxo-1, 3-thiazolidine ring system. The other compounds, **4b-4g** showing good binding interactions, contained an electronegative atom attached to the ortho position on the aromatic ring directly attached to the methyl-oxo-1,3-thiazolidin ring system. The related data of docking studies are given in Table 1.

Table 1. Docking scores of the compounds with binding affinity (Kcal/mol).

S. No.	Code	Structure	Binding Energy (Kcal/mol)	H-Bond	Interacting Amino Acids
1	4a		-7.576	1H	ASN179

2	4b		-7.359	2H	ASN179 PHE110 LEU90 TYR148
3	4c		-6.552	1H	ASN179
4	4d		-6.545	1H	ASN179
5	4e		-6.225	1H	ASN179
6	4f		-6.174	1H	ASN179
7	4g		-6.047	2H	ASN179 TYR148
8	4h		-5.987	No H Bond	ASN179

No.	ID	Structure	Affinity	H-bonds	Residues
9	4i		-5.942	1H	ASN179
10	4j		-5.788	1H	ASN179 PHE110
11	4k		-5.515	1H	ASN179 PHE110 MET102
12	4l		-5.038	No H Bond	ASN179
13		Ciprofloxacin	-6.714	2H	ASN179 TYR148

Molecular dynamic (MD) simulation

MD simulations of the docked poses were performed to understand the dynamic behaviour (stability) of the protein-ligand complex in the physiological environment using GROMACS version 4.5.5. It indicated the binding affinities of different ligands (CPD**4a** and CPD**4b**) with macromolecule protein (3Q3S) in its free and complex form. Isoniazid was the reference with the known stability value when complexed with the protein. The bounded ligand and protein complex (3Q3S with reference ligand, CPD**4a** and CPD**4b)** were analyzed using parameters like RMSD (root mean square deviation), RMSF (root mean square fluctuation), Rg (radius of gyration), SASA (solvent accessible surface area), number of hydrogen bonds, and variation of secondary structure pattern between the protein and their complexes. For a 50 ns simulation duration, four different simulations were run for the protein structure and each of their corresponding complexes. Our results showed that the protein 3Q3S, in both its free and complex forms, reaches equilibrium in around 5 ns, then, after displaying a stable trajectory,

resonates only between 0.10 and 0.2 nm of RMSD until the end of the simulation (Figure 4). The RMSD plot demonstrated that 3Q3S is fairly flexible in its free form and deviates in a reasonable amount, which is demonstrated by its higher RMSD values than its complex form (Figure 4a). This indicated that the backbone of the protein did not change its behaviour in going from the crystal structure to the protein structure in water.
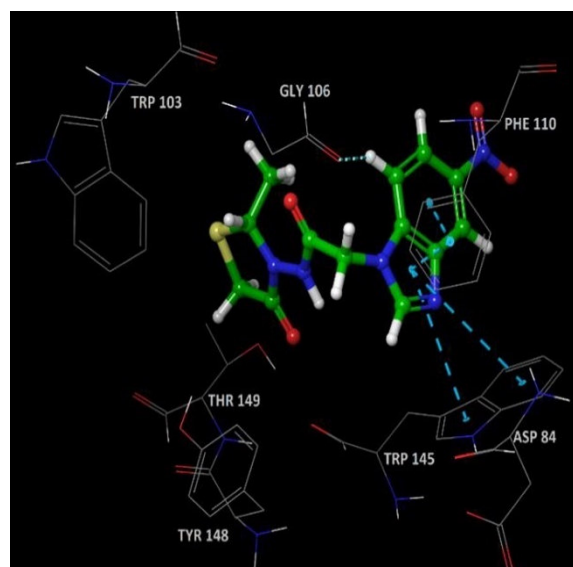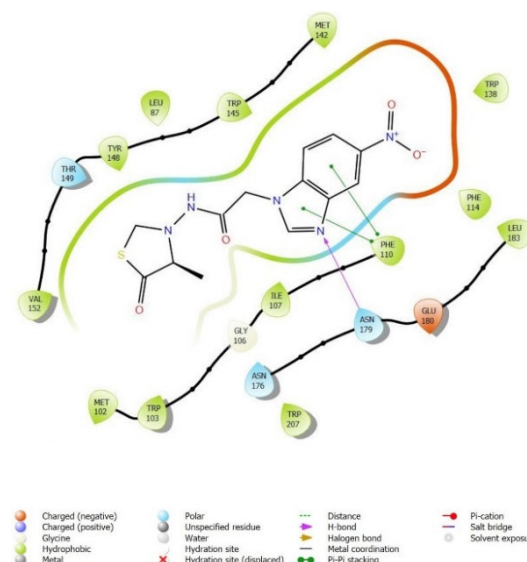

Figure 1 (a)   **Figure 1 (b)**

Figure 1. Docking pose **(1a)** and ligand interaction diagram **(1b)** of *N*-(4-methyl-4-oxo- 1 3-thiazolidin-3-yl)-2-(5-nitro-1*H*-benzimidazol-1-yl) acetamide (**4a**).

Additionally, it was noted that the RMSD of CPD4a in its complex with protein was quite small (0.15-0.20 nm), which indicated that stable complexes would form until the end of the simulation. CPD4b with the protein displayed trajectories, but only minor variations were seen in terms of equilibration time and average RMSD values, even though it reached initial stable equilibration by the simulation's conclusion. Throughout the simulation, every complex tended to reach a steady trajectory; this was supported by the fact that all complexes with a limit of 0.3 nm had higher RMSD. The mass-weighted root means a square distance of each atom from its centre of mass is its radius of gyration. In the plot of Rg, the overall structures during the trajectory can be examined for capability, shape, and folding (Figure 4b). The protein and complex had a consistent trend for the Rg value of 1.95-2.00 nm throughout the simulation.

Moreover, the number of hydrogen bonds created during the simulation between various protein residues and ligands was estimated (Figure 4c). From the graph, it is understood that the hydrogen bonds detected during the MD simulation were formed with the amino acid residues. The number of hydrogen bonds (NH) formed and maintained during the MD simulation was interestingly complementary to the docking results. The variation in the number of hydrogen bonds that ever occurred can only be explained by the dynamic movement of the protein and interacting ligands during the simulation, which may introduce or omit a few hydrogen bonds throughout the simulation.

SASA (solvent accessible surface area) measurements were made to assess the degree of compactness to which the hydrophobic cores formed between distinct protein-ligand complexes (Figure 4d). The results demonstrate a range of SASA values that were seen with several complexes, with the 3Q3S-CPD 4a, CPD 4b complex, and reference ligand showing the highest SASA values (110-120 nm). The C-RMSF is calculated to observe the overall flexibility of atomic positions in the trajectory for the proteins and their complexes, as shown in (Figure 4e. I and e. II). Interestingly, although the C-RMSF values for the 3Q3S protein with CPD 4a and CPD 4b increased, the active site amino acid residues Phe110, Phe119, Met142, Asn176, Asn179, and Thr207 interestingly changed within a very small range, indicating the protein structural conformation was preserved.
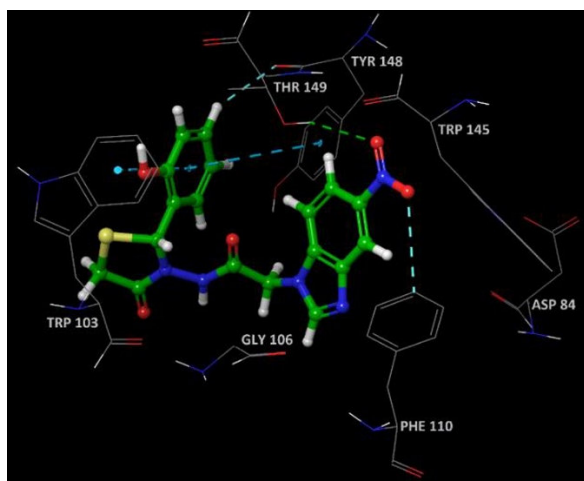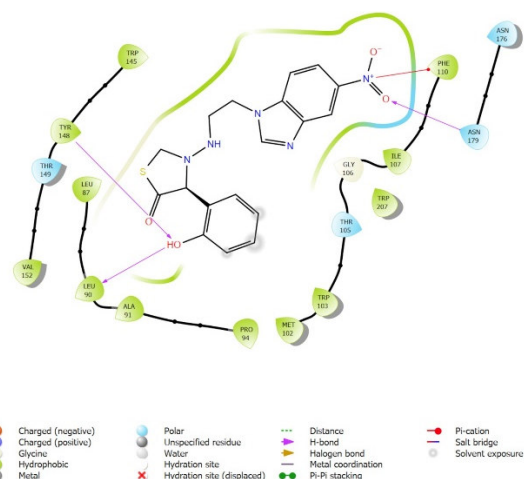
Figure 2a

Figure 2b

Figure 2. Docking pose **(2a)** and ligand interaction diagram **(2b)** of *N*-[4-(2-hydroxyphenyl)-4-oxo-1 3-thiazolidin-3-yl]-2-(5-nitro-1*H*-benzimidazol-1-yl) acetamide(**4b**).
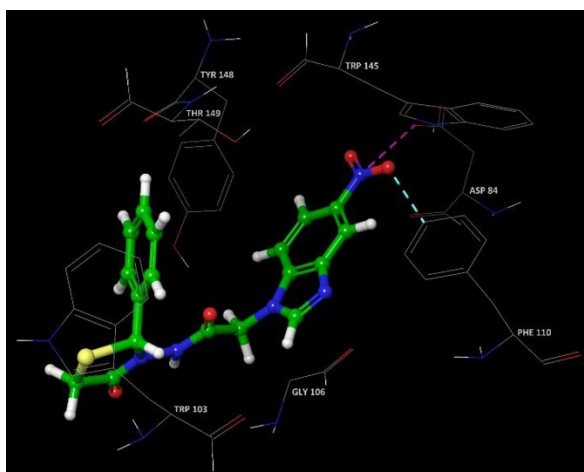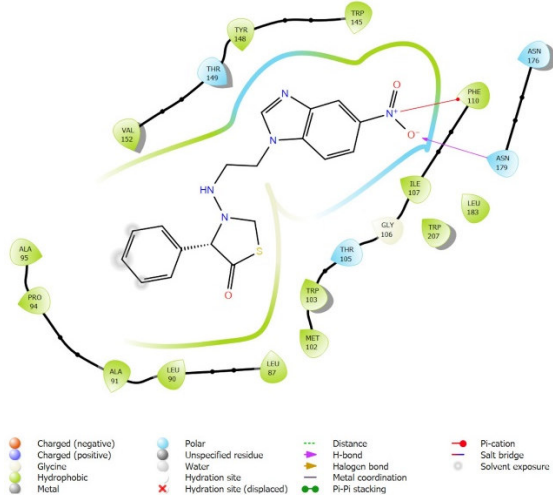

Figure 3a

Figure 3b

Figure 3. Docking pose **(3a)** and ligand interaction diagram **(3b)** of 2-(5-nitro-1*H*-benzimidazol-1-yl)-*N*-(4-oxo-4-phenyl-1 3-thiazolidin-3-yl) acetamide (**4g**).

Table 2. *In-vitro* anti-tubercular activity of the compounds using MAB Assay.

S. No	Compounds	MIC(µg/ml) *M. tuberculosis* H37RV
1	4a	1.6
2	4b	1.6
3	4c	6.25
4	4d	3.125
5	4e	3.125
6	4f	3.125
7	4g	1.6
8	4h	12.5
9	4i	6.25
10	4j	3.125
11	4k	3.125
12	4l	3.125
13	Pyrazinamide	3.125
14	Ciprofloxacin	3.125
15	Streptomycin	6.25

Anti-tubercular activity

The results of the assay in terms of MIC (µg/ml) are given in Table 2. Pyrazinamide, streptomycin and ciprofloxacin were used as standards for comparison. Compounds 4a, 4b, 4g have shown better

activity than the standard drugs with MIC values 1.6 μg/ml and all other compounds also exhibited good activity with MIC values between 3.125-6.25 μg/ml, which is either equivalent to or better than the standards used.
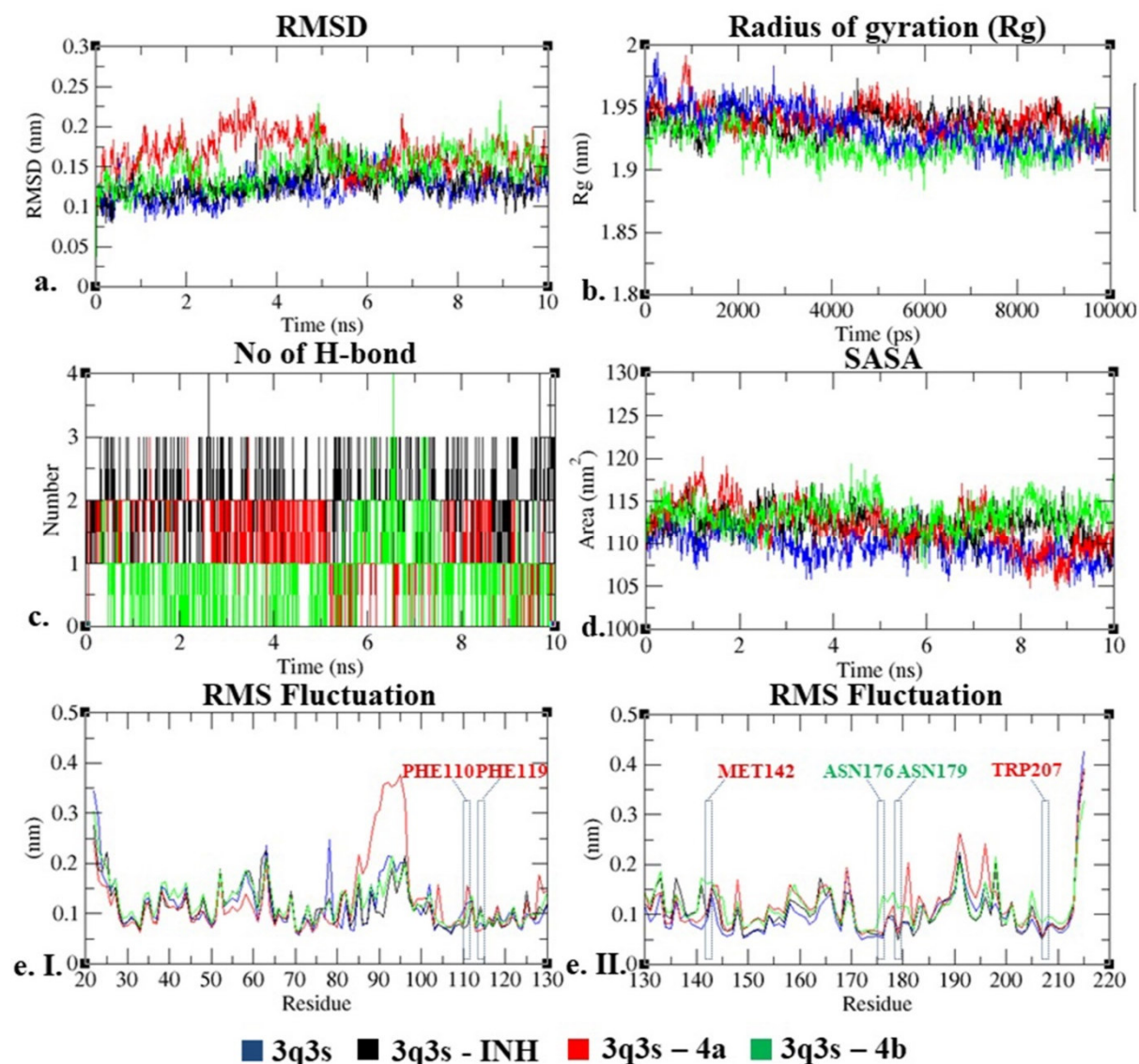

Figure 4. (a) Analysis of 3Q3S_ with Isoniazid (INH) CPD 4a and CPD 4b complexes at 50,000 ps RMSD Rg hydrogen bond SASA and RMSF. Time evolution of the backbone RMSD of the 3Q3S_ protein both by itself and in combination with the INH CPD4a and CPD4b complex structures. (b) The protein backbone's gyrating radius (Rg) in both its free and complex states for the duration of the simulation. Rg (nm) is the ordinate, while time (ps) is the abscissa. (c) Hydrogen bonds forming between several ligands and proteins during the simulation. (d-e) When the ordinate is SASA (nm) and the abscissa is time, SASA is indicated (ps). I and II. Protein and several ligands average RMSF plotted by residue.

Conclusion

A series of novel substituted *N*-(4-alkyl-4-oxo-1,3-thiazolidin-3-yl)-2-(5-nitro-1H-benzimidazole-1-yl) acetamide derivatives were studied for their anti-tubercular activity. The compounds **4a** and **4b**, which have shown the lowest binding energies with transcription inhibitor protein, have shown the best MIC value against *M. tuberculosis* by MABA. The *in-vitro* activity of **4a** and **4b** was better than the standard drugs used for the MABA. The compound **4g**, which has also shown good *in-vitro* activity, has 2 H-bonding interactions with ASN 179. The docking pose of these ligands has shown that binding with ASN 179 is essential for activity along with one or more H-bonding.

Furthermore, molecular simulation studies were carried out to understand the protein-ligand stability, and it was understood that the increased number of H-bonds formed by the synthesized compound 4a having interaction distances less than 3.0 Å gives the structural insight to support the

claim why it was able to bind tightly with the active pocket of the targeted enzyme. Molecular dynamic calculations up to 50ps have shown stability as protein structural conformation was preserved. The substitution of *ortho-substituted* aryl group containing polar substituent is preferred at the 2-thiazolidine ring. This series can give a good anti-TB agent; more modifications can be explored on the ortho-aryl substitution with a polar group.

Acknowledgements

Authors contribution

All the authors have contributed equally.

Declaration of interest

The authors declare no conflict of interest.

References

1. Rangappa SK, Rajappa CK, Patil SA. Nagaraja BM. Benzimidazole-core as an antimycobacterial agent. Pharmacol Rep. 2016;68(6) 1254-65.
2. https://www.who.int/news-room/fact-sheets/detail/tuberculosis. [cited 2022 Oct 19].
3. Yadav G, Ganguly S. Structure activity relationship (SAR) study of benzimidazole scaffold for different biological activities: A mini-review. Eur J Med Chem. 2015;97:419-43.
4. Migliori GB, Tiberi S. WHO drug-resistant TB guidelines 2022: what is new? [cited 2022 Oct 19]. Available From: https://www.ingentaconnect.com/contentone/iuatld/ijtld/2022/00000026/00000007/art00004?crawler=true&mimetype=application/pdf
5. Dover LG, Coxon GD. Current status and research strategies in tuberculosis drug development. J. Med Chem. 2011;54(18):6157-65.
6. Lemura R, Kawashima T, Fukuda T, Lto K, Tsukamoto G. Synthesis of 2-(4-Substituted-l-piperazinyl)benzimidazole as H1-Antihistaminic Agents. J Med Chem. 1986;29(7): 1178-83.
7. Noor A, Qazi NG, Nadeem H, Khan AU, Paracha RZ, Ali F, et al. Synthesis characterization anti-ulcer action and molecular docking evaluation of novel benzimidazole-pyrazole hybrids. Chem Cent J. 2017;11:1-13.
8. Desai NC, Shihory NR, Kotadiya GM, Desai P. Synthesis antibacterial and antitubercular activities of benzimidazole bearing substituted 2-pyridone motifs. Eur J Med Chem. 2014;82:480-9.
9. Ayhan-Kilcigil G, Kus C, Çoban T, Can-Eke B, Iscan M. Synthesis and antioxidant properties of novel benzimidazole derivatives. J Enzyme Inhib Med Chem. 2004;19(2) 129-35.
10. Valdez J, Cedillo R, Hernández-Campos A, Yépez L, Hernández-Luis F, Navarrete-Vázquez G, et al. Synthesis and antiparasitic activity of 1H-benzimidazole derivatives. Bioorganic Med Chem Lett. 2002;12(16): 2221-4.
11. Rajasekaran S, Gopalkrishna AC. Synthesis anti-inflammatory and anti-oxidant activity of some substituted benzimidazole derivatives. Int J Drug Dev Res. 2012;4(3):303-9.
12. Tupe AP, Pawar PY, Mane BY, Magar SD. Synthesis analgesic and anti-inflammatory activity of some 2-substitued 3-acetic acid benzimidazole derivatives. Res J Pharm Biol Chem Sci. 2013;4(2):928-35.
13. Özkay Y, Tunalı Y, Karaca H, Işıkdağ I. Antimicrobial activity of a new series of benzimidazole derivatives. Arch Pharm Res. 2011;34(9):1427-35.
14. Torres-Gómez H, Hernández-Núñez E, León-Rivera I, Guerrero-Alvarez J, Cedillo-Rivera R, Moo-Puc R, et al. Design synthesis and in vitro antiprotozoal activity of benzimidazole-pentamidine hybrids. Bioorg Med Chem Lett. 2008;18(11):3147-51.
15. Sharma MC, Kohli DV, Sharma S, Sharma AD. Synthesis and antihypertensive activity of some new benzimidazole derivatives of 4'-(6-methoxy-2-substituted-benzimidazole-1-ylmethyl)- biphenyl-2-carboxylic acid in the presences of BF3. OEt2. Der Pharm Sin. 2010;1(1):104-115.
16. Baszczak-Swiatkiewicz K, Olszewska P, Mikiciuk-Olasik E. Biological approach of anticancer activity of new benzimidazole derivatives. Pharmacol Rep. 2014;66(1):100-6.
17. Yadav P, Deolekar P, Kanase V, Mishra S. Overview of new Anti TB drugs. IJPSR. 2012;3(8):2472-81.
18. Desai NC, Dodiya AM, Makwana AH. Antimicrobial screening of novel synthesized benzimidazole nucleus containing 4-oxo-thiazolidine derivatives. Med Chem Res. 2012;21:2320-8.
19. Klimesová V, Kocí J, Waisser K, Kaustová J. New benzimidazole derivatives as antimycobacterial agents. Farmaco. 2002;57(4):259-65.

20. Jain AK, Vaidya A, Ravichandran V, Kashaw SK, Agrawal RK. Recent developments and biological activities of thiazolidinone derivatives: A review. Bioorg Med Chem. 2012;20(11):3378-95.

21. Bjelkmar P, Larsson P, Cuendet MA, Hess B, Lindahl E. Implementation of the CHARMM force field in GROMACS: analysis of protein stability effects from correction maps virtual interaction sites and water models. J Chem Theory Comput. 2010;6(2): 459-66.

22. Mark P, Nilsson L. Structure and dynamics of the TIP3P SPC and SPC/E water models at 298 K. J Phys Chem A. 2001;105:9954-60.

23. Nosé S, Klein ML. Constant pressure molecular dynamics for molecular systems. Mol Phys. 1983;50(5):1055-76.

24. URL: https://plasma-gate.weizmann.ac.il/pub/grace. [Cited: 2023 June 26].

25. Dubey S, Bhardwaj S. Synthesis of some novel benzimidazole-oxothiazolidine derivatives as anti-tubercular agents: conventional vs microwave assisted approach. Research J Science and Tech. 2022;14(4):199-207.